

RETHINKING SELF-SUPERVISED VISUAL REPRESENTATION LEARNING IN PRE-TRAINING FOR 3D HUMAN POSE AND SHAPE ESTIMATION

Hongsuk Choi^{*†1,2}, Hyeongjin Nam^{*2}, Taeryung Lee², Gyeongsik Moon³, Kyoung Mu Lee^{2,4}

¹Samsung Research America, New York

²Dept. of ECE & ASRI, Seoul National University, Korea

³Meta Reality Labs Research

⁴IPAI, Seoul National University, Korea

ABSTRACT

Recently, a few self-supervised representation learning (SSL) methods have outperformed the ImageNet classification pre-training for vision tasks such as object detection. However, its effects on 3D human body pose and shape estimation (3DHPSE) are open to question, whose target is fixed to a unique class, the human, and has an inherent task gap with SSL. We empirically study and analyze the effects of SSL and further compare it with other pre-training alternatives for 3DHPSE. The alternatives are 2D annotation-based pre-training and synthetic data pre-training, which share the motivation of SSL that aims to reduce the labeling cost. They have been widely utilized as a source of weak-supervision or fine-tuning, but have not been remarked as a pre-training source. SSL methods underperform the conventional ImageNet classification pre-training on multiple 3DHPSE benchmarks by 7.7% on average. In contrast, despite a much less amount of pre-training data, the 2D annotation-based pre-training improves accuracy on all benchmarks and shows faster convergence during fine-tuning. Our observations challenge the naive application of the current SSL pre-training to 3DHPSE and relight the value of other data types in the pre-training aspect.

1 INTRODUCTION

Transferring the knowledge contained in one task and dataset to solve other downstream tasks (*i.e.*, transfer learning) has proven very successful in a range of computer vision tasks (Girshick et al., 2014; Carreira & Zisserman, 2017; He et al., 2017). In practice, transfer learning is done by pre-training a backbone (He et al., 2016) on source data to learn better visual representations for the target task. The ImageNet classification has been the de facto pre-training paradigm in computer vision, and the 3D human body pose and shape estimation (3DHPSE) literature has followed this.

Recently, self-supervised representation learning (SSL) has gained popularity in the interest of reducing labeling costs (Chen et al., 2020a; Grill et al., 2020; He et al., 2020; Caron et al., 2020; Hénaff et al., 2021). SSL pre-trains a backbone using unlabeled arbitrary object images and fine-tunes the backbone on target tasks. MoCo (He et al., 2020) and DetCon (Hénaff et al., 2021) surpassed the ImageNet classification pre-training for downstream tasks like object detection and instance segmentation on arbitrary class objects. Motivated by them, PeCLR (Spurr et al., 2021) and HanCo (Zimmermann et al., 2021) targeted a human hand and pre-trained a backbone on hand data without 3D labels. They showed the accuracy improvement for 3D hand pose and shape estimation from the controlled setting (Zimmermann et al., 2019), compared with random initialization (no pre-training) and the ImageNet classification pre-training. While the results of PeCLR and HanCo are promising for 3DHPSE, they have limited practical lessons. For example, the amounts of labeled hand data, which is fine-tuning data, are significantly smaller ($\sim 64\text{K}$) than that of the commonly used labeled body data ($\sim 480\text{K}$). Also, the total training (pre-training&fine-tuning) time of the different

^{*}equal contribution.

[†]Most work was done when Hongsuk Choi was at Seoul National University.

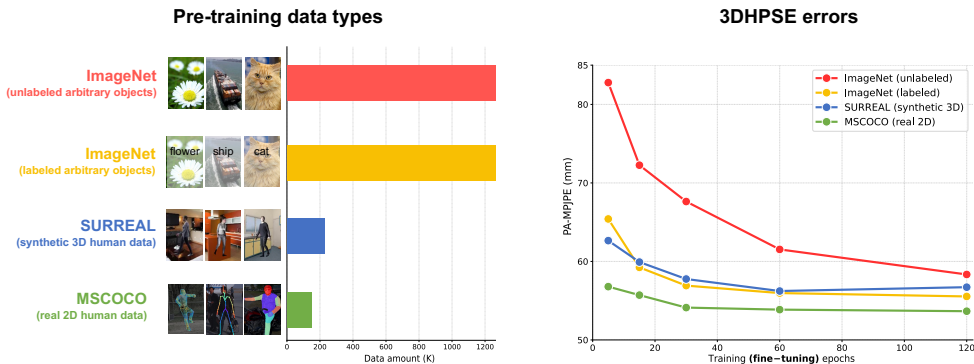


Figure 1: (Left) We pre-train a backbone (ResNet-50 (He et al., 2016)) with different data types: unlabeled arbitrary objects (Russakovsky et al., 2015), labeled arbitrary objects (Russakovsky et al., 2015), synthetic 3D human data (Varol et al., 2017), and real 2D human data (Lin et al., 2014). (Right) 3DHPSE errors when initializing its backbone with differently pre-trained weights. We fine-tune PARE (Kocabas et al., 2021) on Human3.6M (Ionescu et al., 2014) and MSCOCO (Lin et al., 2014) and evaluate it on 3DPW (von Marcard et al., 2018).

approaches is not matched, which is critical to the final accuracy (He et al., 2019). Last, they require labeled data with bounding boxes of a hand.

This paper questions the effectiveness of SSL pre-training for 3DHPSE by thoroughly comparing with alternatives in multiple aspects (*i.e.* final accuracy, convergence speed, and cost-effectiveness). We perform experiments by fixing the fine-tuning task to 3DHPSE and changing the pre-training approach. The experiments are organized in three steps. First, we compare state-of-the-art SSL methods, pre-trained on ImageNet, with the ImageNet classification pre-training. Different object detection and instance segmentation, the SSL methods are outperformed by the classification pre-training in three 3DHPSE benchmarks with 7.7% margin on average. Interestingly, the accuracy of SSL is comparable to or even worse than the random initialization baseline. The results imply general visual representations learned by SSL could be detrimental to 3DHPSE.

Second, we explore the reasons behind the current SSL methods’ disappointing performance in depth by contriving a new pre-training approach. Modern SSL pre-training methods (Chen et al., 2020a; He et al., 2020) have two unfavorable factors on 3DHPSE; 1) they learn inconsistent representations for the same class instances as argued by (Khosla et al., 2020), which hinders learning high-level priors about a specific class, and 2) SSL pre-training has an instance-level learning characteristic (*i.e.*, a single attribute per image), which has an inherent task gap with 3DHPSE that requires understanding of the fine-level semantic information (*i.e.*, multiple attributes per image), the human joints. We combine an SSL approach with 2D joint labels, which we call JointCon, to experimentally validate the two factors’ effects. JointCon contrasts local image features of human joints instead of global image features of images.

Third, we compare SSL methods with 2D annotation-based pre-training and synthetic data pre-training on human data following PeCLR (Spurr et al., 2021) and HanCo (Zimmermann et al., 2021), and discuss cost-effectiveness in Section 5 and B. 2D annotation-based pre-training and synthetic data pre-training are worth investigating in that they share the motivation of SSL, which is to benefit from data¹ with less collection cost (Rong et al., 2019; Patel et al., 2021). In our experiments on human data, 2D annotation-based pre-training shows the highest accuracy and the fastest convergence speed among different pre-training approaches. Compared with the classification baseline, its final accuracy is increased by 3.1% on 3DPW (von Marcard et al., 2018) and 1.9% on Human3.6M (Ionescu et al., 2014). In 3DPW, the convergence speed is approximately 2× faster. In the semi-supervised setting, the accuracy improvement increases to 9.9% on 3DPW and 7.1% on Human3.6M. We assume rich pose and appearance information learned from the 2D pose data is the key to these improvements as expected. Synthetic data pre-training produces higher errors than the classification baseline. We conjecture that a domain gap between real and synthetic data inter-

¹Unless otherwise noted, ‘data’ indicates labeled images

rupts efficient transfer learning. Finally, SSL on human data also underperforms the classification pre-training. The overall results of SSL suggest that the current stage of SSL may not be enough to benefit 3DHPSE, which essentially requires high-level understanding of human kinematic structure.

Our main empirical results are summarized in Figure 1. The current SSL that pre-trains on unlabeled arbitrary object images is not effective for 3DHPSE. Despite the least amount of pre-training data, 2D annotation-based pre-training provides the best result. This paper has two significant empirical contributions; 1) we provide novel experimental evidence and discussion points for people to rethink the naive application of SSL pre-training paradigm in 3DHPSE, and 2) we rehighlight the value of other data types that have received relatively less attention in the pre-training aspect.

2 RELATED WORK

3D human pose and shape estimation. We focus on reviewing the body, not hand literature, where extensive works have been addressed for 3D pose and shape estimation from in-the-wild images. HMR (Kanazawa et al., 2018) proposed an end-to-end trainable human mesh recovery system that introduced adversarial loss to leverage MoCap data without images. GraphCMR (Kolotouros et al., 2019b) designed a graph convolutional network that takes the rest pose human mesh and image features as input and predicts mesh vertex coordinates. SPIN (Kolotouros et al., 2019a) combined a neural network regressor (Kanazawa et al., 2018) and an iterative fitting framework (Bogo et al., 2016). I2L-MeshNet (Moon & Lee, 2020) introduced a *lixel*-based 1D heatmap to estimate mesh vertex coordinates. Pose2Mesh (Choi et al., 2020) proposed a graph convolutional network that recovers 3D human pose and mesh from a 2D human pose. VIBE (Kocabas et al., 2020) and TCMR (Choi et al., 2021) extended HMR to video input. METRO (Lin et al., 2021) improved GraphCMR (Kolotouros et al., 2019b) with a transformer architecture. PARE (Kocabas et al., 2021) introduced a part-guided attention mechanism for mesh parameter regression. PyMAF (Zhang et al., 2021a) used mesh-aligned image features to iteratively refine prediction. 3DCrowdNet (Choi et al., 2022) resolved the inter-person occlusion issue in crowded scenes with 2D pose guidance for image features and a joint-based regressor (Moon et al., 2022a).

Human dataset. Human datasets for 3DHPSE can be broadly categorized into three types; Motion capture (MoCap) dataset, in-the-wild 2D dataset, and synthetic dataset. MoCap datasets (Ionescu et al., 2014; Mehta et al., 2017) provide accurate 3D joint labels with images captured from a controlled multi-view studio. In-the-wild 2D datasets (Andriluka et al., 2014; Johnson & Everingham, 2010) contain manually annotated 2D labels, which are usually 2D joints. MSCOCO (Lin et al., 2014) is the most widely used dataset that has rich 2D annotations, including part segmentation and DensePose (Güler et al., 2018). Synthetic datasets (Varol et al., 2017; Patel et al., 2021) render 3D human avatars on synthetic background images. Human poses from MoCap data and appearances from real scan data are exploited. Recent works (Patel et al., 2021; Baradel et al., 2021; Cai et al., 2021) have shown that fine-tuning on synthetic human data can improve accuracy on real-world benchmarks. 3DPW (von Marcard et al., 2018) is an in-the-wild human benchmark with 3D body pose and mesh annotations. Since few in-the-wild 3D human datasets exist, evaluation on 3DPW is the current best way to evaluate 3DHPSE methods on in-the-wild images.

The concurrent work of (Pang et al., 2022) provides experimental results on pre-training on three datasets (classification on ImageNet, 2D pose estimation on MPII (Andriluka et al., 2014) and MSCOCO). However, the effects of SSL and synthetic data are still unexplored. Considering that SSL has shown a powerful impact on other vision tasks, the extensive experiments and analysis on the current SSL methods distinguish our work from (Pang et al., 2022).

Self-supervised representation learning. Recently, contrastive learning-based methods are showing state-of-the-art performance among self-supervised approaches. The contrastive learning’s fundamental idea is to pull together an anchor and a “positive” sample in embedding space, and to push apart the anchor from many “negative” samples (Khosla et al., 2020). Since this strategy can be applied to unlabeled training data, assuming a positive pair from data augmentations of the same sample, the research community has endeavored to use the learned representation for downstream transfer tasks. In practice, a backbone is pre-trained on a large-scale classification dataset (Rusakovsky et al., 2015; Mahajan et al., 2018) without using labels, and fine-tuned for classification, object detection, or instance segmentation.

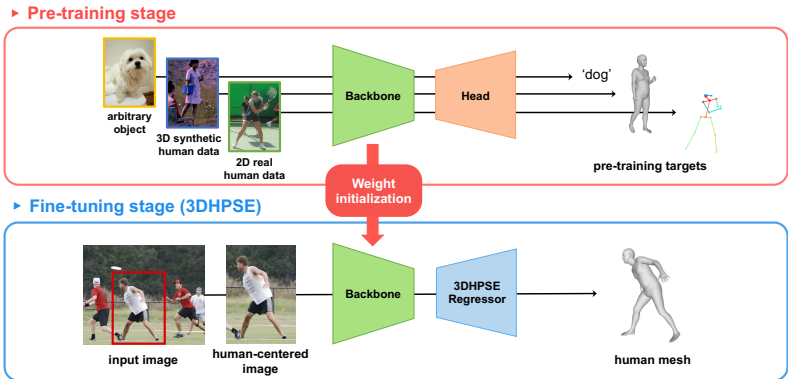


Figure 2: Overview of the training procedure for 3DHPSE. We pre-train a backbone with each different data type (e.g., labeled arbitrary object, synthetic 3D human data, and real 2D human data). From the pre-trained backbone, we fine-tune both the backbone and a human mesh regressor in an end-to-end manner.

MoCo (He et al., 2020; Chen et al., 2020c) interpreted the contrastive learning as building a dynamic and large dictionary of embeddings with a queue and a moving-averaged key encoder. SimCLR (Chen et al., 2020a;b) introduced a nonlinear projection layer and proved that augmentation during pre-training should be stronger than supervised learning. SwAV (Caron et al., 2020), SiamSiam (Chen & He, 2020), and BYOL (Grill et al., 2020) eliminated the requirements for negative samples, while maintaining the Siamese architecture. DetCon (Hénaff et al., 2021) proposed a new contrastive objective that is based on unsupervised mask generation.

PeCLR (Spurr et al., 2021) and HanCo (Zimmermann et al., 2021) are the recent works that adapted SSL to 3D hand pose and shape estimation. PeCLR proposed a contrastive objective equivariant to geometric transformations (e.g., rotation and translation), which models the transformations in a latent vector level similar to (Rhodin et al., 2018) and NSD (Rhodin et al., 2019). It showed accuracy improvements over the random initialization baseline, but trained on a small-scale dataset ($\sim 32K$) (Zimmermann et al., 2019) during fine-tuning, although more hand data, for example, MSCOCO (150K) and YT3D (47K), exists. HanCo applied MoCo (He et al., 2020) on a background-augmented unlabeled hand dataset, but the improvement was marginal and like PeCLR, experiments were done in the controlled setting, not the in-the-wild environment.

3 CONVENTION OF 3D HUMAN POSE AND SHAPE ESTIMATION

Architecture. A 3DHPSE network consists of a backbone and a human mesh regressor, as depicted in Figure 2. A backbone (He et al., 2016; Sun et al., 2019) extracts image features from a given human-centered image. The features are fed to a human mesh regressor that estimates a mesh defined by human models, such as SMPL (Loper et al., 2015).

Pre-training. Almost all 3DHPSE methods pre-train their backbones by ImageNet (Russakovsky et al., 2015) classification. They take pre-trained weights from the open source (e.g., torchvision (Paszke et al., 2017)) and initialize their backbones with them in practice. Initializing a backbone’s weights with the ImageNet classification-pre-trained weights is known to expedite training convergence and to bring better accuracy than random initialization.

Fine-tuning. During fine-tuning, a pre-trained backbone and a human mesh regressor are trained in an end-to-end manner by mix-using MoCap and in-the-wild 2D datasets. 2D annotations of in-the-wild 2D datasets weakly supervise the 3D mesh prediction (Kanazawa et al., 2018), and the 3D pseudo-mesh labels generated from 2D joints (Pavlakos et al., 2019; Joo et al., 2021; Moon et al., 2022b) directly supervise the 3D output. The mixed use of the MoCap and the in-the-wild 2D datasets has enabled reasonable performance on in-the-wild 3DHPSE, despite the scarce in-the-wild 3D training data.

4 EXPERIMENT

4.1 SETTING

We adopt ResNet-50 (He et al., 2016) as a backbone and a SMPL (Loper et al., 2015) mesh as an estimation target. During fine-tuning on 3DHPSE, we mainly use PARE (Kocabas et al., 2021) as a human mesh regressor and Human3.6M (Ionescu et al., 2014) and MSCOCO (Lin et al., 2014) as training datasets. For the semi-supervised setting, we exploit 10% of Human3.6M and 10% of MSCOCO data. 3DPW (von Marcard et al., 2018), Human36M (Ionescu et al., 2014), and MuPoTS-3D (Mehta et al., 2018) are used as evaluation benchmarks. We report PA-MPJPE for 3DPW, Human36M, and 3DPCK for MuPoTS-3D following the convention. PA-MPJPE stands for the Procrustes-aligned mean per-joint position error in millimeters. 3DPCK indicates the percentage of correct 3D keypoints.

Pre-training. For the SSL pre-training on ImageNet (Chen et al., 2020b; Chen & He, 2020; Caron et al., 2020; Chen et al., 2020c; Hénaff et al., 2021), we use the publicly released pre-trained ResNet-50 weights. SSL pre-training on ImageNet typically requires much larger computational costs to be effective than the classification baseline. For pre-training on human datasets, we fix the pre-training length (total number of training epochs) at 140 epochs regardless of methods, which is longer than those of 3DHPSE adapted SSL papers (100 epochs) (Spurr et al., 2021; Zimmermann et al., 2021) and the same as that of (Xiao et al., 2018). To pre-train the proposed 2D pose-driven alternatives, we decay the learning rate by $10\times$ at 90 and 120 epochs, starting from the initial value of 10^{-3} following (Xiao et al., 2018).

Fine-tuning. For fine-tuning, we train a 3DHPSE network for 120 epochs and decay the learning rate by $10\times$ at 90 epochs, which is originally 10^{-4} . This schedule empirically showed full convergence for various networks initialized with different pre-trained weights. For the case of training from scratch (*i.e.*, random initialization), following the spirit of (He et al., 2019), we extend the total training length to 240 epochs and decay the learning rate by $10\times$ at 180 epochs from 10^{-4} . It roughly matches the total training length of the pre-training counterparts (140 epochs + 120 epochs) and empirically showed full convergence.

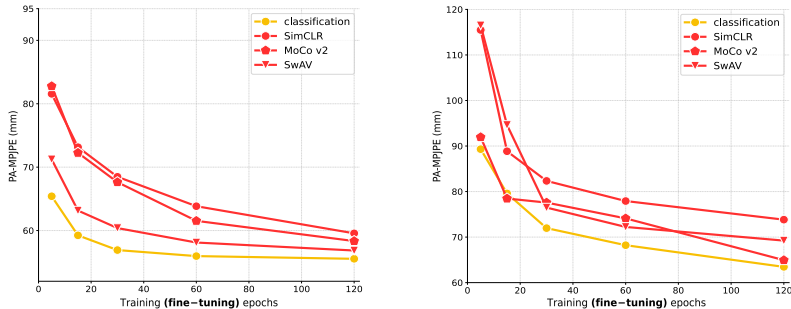
4.2 PRE-TRAINING ON IMAGENET

We first examine the effects of the current state-of-the-art SSL methods (Chen et al., 2020b; Chen & He, 2020; Caron et al., 2020; Chen et al., 2020c; Hénaff et al., 2021) that pre-train a backbone on ImageNet. As summarized in Table 1 and Figure 3, when full fine-tuning data is used, they show approximately $2\times$ slower convergence and 7.7% higher errors (PA-MPJPE) than the ImageNet classification pre-training (He et al., 2016). Interestingly, the final accuracy is even worse than the random initialization baseline, though the convergence is faster. In the semi-supervised setting, SSL methods outperform the random initialization baseline by 2.5%, but still the classification pre-training provides the best overall accuracy.

We analyze the results that seemingly oppose the fact that SSL surpasses the random initialization and classification baselines in object detection and instance segmentation (Grill et al., 2020; Hénaff et al., 2021) by answering three questions. (i) ***Why SSL is worse than the random initialization baseline, when full fine-tuning data is used?*** We conjecture that a data domain gap is one of the reasons for the different results. While both object detection and instance segmentation target localization of arbitrary class objects, 3DHPSE only targets a single class, the human. For inference on arbitrary class objects, learning a wide range of general features unlimited to labels of a dataset could be advantageous in the generalization aspect (Tendle & Hasan, 2021). However, for 3DHPSE, a backbone network is preferred to learn more about human features rather than features of arbitrary objects, given the limited learning capacity. Transferring knowledge about arbitrary objects could distract a network from learning necessary human features for 3DHPSE. (ii) ***Why the classification pre-training outperforms the random initialization baseline, while SSL does not, when full fine-tuning data is used?*** The classification pre-training makes a backbone to learn high-level semantic representations, such as the global structure of objects, that could be beneficially transferred to inference on humans. For example, (Yosinski et al., 2015) showed that AlexNet (Krizhevsky et al., 2017) trained on ImageNet can recognize important features of human faces, although ImageNet has no labels of human faces. On the contrary, visual representations learned by SSL are likely to lack high-

Table 1: Effects of self-supervised pre-training on ImageNet. The red and blue colors indicate the first and second best scores, respectively.

fine-tuning data	pre-training data	pre-training method	3DPW	H36M	MuPoTS
			PA-MPJPE↓	PA-MPJPE↓	3DPCK↑
H36M+ MSCOCO (100%)	-	random init.	56.37	52.72	67.12
	ImageNet (labeled)	classification	55.65	48.36	67.76
	ImageNet (unlabeled)	SimCLR (Chen et al., 2020a;b)	59.56	56.93	65.67
		SimSiam (Chen & He, 2020)	56.42	51.82	66.34
		SwAV (Caron et al., 2020)	56.85	52.18	66.19
		MoCo v2 (Chen et al., 2020c)	58.34	55.43	66.68
		DetCon (Hénaff et al., 2021)	64.54	58.83	63.83
H36M+ MSCOCO (10%)	-	random init.	73.37	67.59	57.32
	ImageNet (labeled)	classification	63.29	58.79	62.75
	ImageNet (unlabeled)	SimCLR (Chen et al., 2020a;b)	73.97	72.02	59.80
		SimSiam (Chen & He, 2020)	66.94	62.45	63.34
		SwAV (Caron et al., 2020)	68.96	63.26	60.79
		MoCo v2 (Chen et al., 2020c)	64.76	60.70	63.47
		DetCon (Hénaff et al., 2021)	81.63	82.60	55.03

Figure 3: Learning curves of PA-MPJPE on 3DPW in the fine-tuning stage when using full fine-tuning data (Left) and 10% of fine-tuning data (Right). The backbone is initialized with different weights pre-trained on **ImageNet** by different pre-training methods.

level information that can be found in objects with the same class. Instead, SSL focuses on learning representations that are invariant to data augmentations, which are performed on a single object sample. These representations can be inconsistent over instances of the same class (Khosla et al., 2020). Considering that 3DHPSE essentially requires high-level priors that are shared across different human samples, inconsistent representations learned by SSL could be detrimental to 3DHPSE. (iii) **Why SSL is effective in the semi-supervised setting, compared with the random initialization?** Inconsistent representations learned by SSL could be a problem for 3DHPSE, but it does not indicate their representations are obsolete. A convolutional neural network requires sufficient training data to extract meaningful low-level features (e.g., textures) from images. In this perspective, insufficient training images deprive a network of learning high-level representations, which in turn harms 3DHPSE. In such a circumstance, SSL can step in to provide a sufficient amount of training images to a network and to make it learn necessary features.

4.3 ANALYSIS OF SSL FOR 3DHPSE.

We further investigate the reasons for the SSL’s disappointing performance discussed in Section 4.2, with experimental evidence. We devise a new pre-training approach, JointCon, that combines the SSL approach with the 2D annotation-based approach. JointCon extracts joint-level features (Moon et al., 2022a) by sampling image features based on GT 2D joint locations. It applies contrastive learning in the joint-level features to pull together an anchor with “positive samples” and push

Table 2: Effects of different representation-level in pre-training via ablation study on JointCon. We use MSCOCO for pre-training. The red and blue colors indicate the first and second best scores, respectively.

fine-tuning data	variations of JointCon	3DPW	H36M	MuPoTS
		PA-MPJPE↓	PA-MPJPE↓	3DPCK↑
H36M+ MSCOCO (100%)	JointCon(I): instance-level	58.29	53.17	67.06
	JointCon(J): joint-level	54.25	45.52	68.87
	JointCon(I+J): instance-level + joint-level	56.71	47.99	67.85
H36M+ MSCOCO (10%)	JointCon(I): instance-level	67.71	62.04	62.64
	JointCon(J): joint-level	57.19	54.97	67.98
	JointCon(I+J): instance-level + joint-level	59.59	56.55	67.38

apart the anchor from “negative samples”. We design three variations of JointCon as below: 1) **JointCon(I)** defines “positive samples” as joint-level features extracted from the same image and “negative samples” as those from different images. 2) **JointCon(J)** defines “positive samples” as joint-level features extracted from the same joint label and “negative samples” as those from different labels. Note that it treats joint-level features of the same joint class from different images as “positive samples”. 3) **JointCon(I+J)** defines “positive samples” as joint-level features extracted from the same image and the same joint label, and “negative samples” otherwise.

Table 2 shows that JointCon(J) outperforms the other variations in all three benchmarks. The accuracy gap between JointCon(J) and JointCon(I+J) proves that it is important to learn consistent representations across instances of the same class. Contrasting representations of the instances in the same class (*i.e.*, objects or joints in the same class) hinders a backbone from learning useful high-level priors and degrades the performance of 3DHPSE. As a result, the ImageNet classification pre-training rather learns consistent representations of the instances in the same class and achieves better accuracy than SSL, as shown in Table 1. The other important observation is that both JointCon(J) and JointCon(I+J) outperform JointCon(I). The accuracy boost by simply adding joint information to the SSL system demonstrates that the current SSL’s low performance is due to the instance-level learning characteristic rather than network architecture, data augmentation, or losses.

4.4 PRE-TRAINING ON A HUMAN DATASET

We investigate three pre-training approaches, SSL, 2D annotation-based pre-training, and synthetic data pre-training. First of all, given the results of Section 4.2, we apply SSL on a human dataset following (Spurr et al., 2021; Zimmermann et al., 2021). PeCLR (Spurr et al., 2021) that adapted SimCLR (Chen et al., 2020a;b) to a 3D hand pose and shape estimation, MoCo v2 (Chen et al., 2020c), the method used by HanCo (Zimmermann et al., 2021), and Swav (Caron et al., 2020), which is not based on contrastive learning, are experimented. MSCOCO (Lin et al., 2014) is used as a pre-training dataset. For synthetic data pre-training, we pre-train PARE (Kocabas et al., 2021) on AGORA (Patel et al., 2021) and SURREAL (Varol et al., 2017). For 2D annotation-based pre-training, we experiment with part segmentation estimation, DensePose (Güler et al., 2018) estimation, and 2D pose estimation on MSCOCO.

As shown in Table 3 and Figure 4, the SSL methods bring faster convergence, but the final accuracy becomes on par with the random initialization baseline. It is also lower than the traditional classification pre-training. SSL appears to be effective only when significantly less fine-tuning data (10% Human3.6M + 10% MSCOCO, < 50K) is used. The results coincide with the experimental results of PeCLR and HanCo; PeCLR was fine-tuned on ~ 32 K labeled data (Zimmermann et al., 2019), and HanCo was fine-tuned on ~ 64 K labeled data (Zimmermann et al., 2021). Synthetic data pre-training shows a similar tendency with SSL, though it outperforms SSL. On the contrary, 2D annotation-based pre-training improves accuracy against the random initialization and classification baselines on all benchmarks. In the semi-supervised setting, the improvement increases up to 12.4% compared with the random initialization. The convergence speed is much faster than both random initialization and classification, especially in the semi-supervised setting.

Table 3: Effects of different pre-training schemes on a human dataset. The red and blue colors indicate the first and second best scores, respectively.

fine-tuning data	pre-training data	pre-training method	3DPW	H36M	MuPoTS	
			PA-MPJPE↓	PA-MPJPE↓	3DPCK↑	
H36M+ MSCOCO (100%)	-	random init.	56.37	52.72	67.12	
	ImageNet (labeled)	classification	55.65	48.36	67.76	
	MSCOCO (unlabeled)	PeCLR (Spurr et al., 2021)	57.27	49.84	66.88	
			MoCo v2 (Chen et al., 2020c)	56.35	50.06	66.95
			SwAV (Caron et al., 2020)	58.20	56.50	66.77
	AGORA SURREAL	3DHPSE	56.77	51.96	67.80	
			56.45	52.51	67.65	
	MSCOCO	part segmentation est.	54.37	48.25	68.55	
			DensePose est.	54.16	49.18	68.43
			2D pose est.	53.34	44.89	69.04
H36M+ MSCOCO (10%)	-	random init.	73.37	67.59	57.32	
	ImageNet (labeled)	classification	63.29	58.79	62.75	
	MSCOCO (unlabeled)	PeCLR (Spurr et al., 2021)	71.24	66.58	60.16	
			MoCo v2 (Chen et al., 2020c)	66.93	62.06	61.36
			SwAV (Caron et al., 2020)	75.98	73.83	58.40
	AGORA SURREAL	3DHPSE	64.71	63.17	65.73	
			62.51	59.10	64.50	
	MSCOCO	part segmentation est.	56.80	54.10	67.69	
			DensePose est.	57.33	54.46	68.02
			2D pose est.	56.92	55.31	67.12

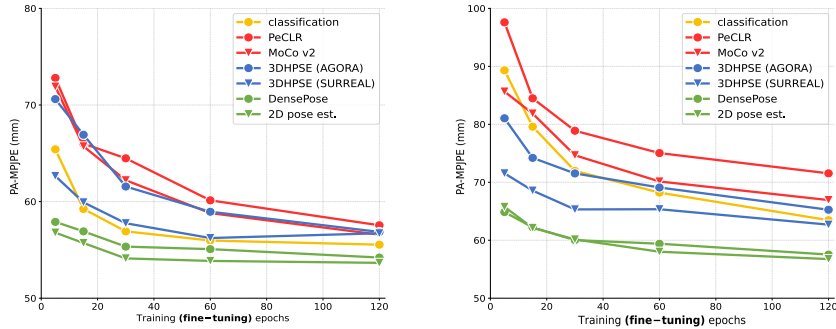


Figure 4: Learning curves of PA-MPJPE on 3DPW in the fine-tuning stage when using full fine-tuning data (Left) and 10% of fine-tuning data (Right). The backbone is initialized with different weights pre-trained on a **human dataset** by different pre-training methods.

We think the results of SSL on human data support the statement in Section 4.2 that representations learned by SSL are hard to embed high-level information related to humans. Synthetic data pre-training has potential to benefit from rich pose and appearance diversity, but a domain gap problem from highly different image appearances between synthetic and real images seems to remain. Compared with SSL and synthetic data pre-training, 2D annotation-based pre-training appears to effectively transfer high-level priors of humans, such as body articulation, to 3DHPSE. Well-aligned 3D body pose and robustness to occlusion in Figure 5 verify the effectiveness of 2D annotation-based pre-training. Figure 6 visualizes each human part’s feature activation of PARE (Kocabas et al., 2021) to further inspect how representations learned by each pre-training approach affect the human mesh regressor’s understanding of human geometry.

5 DISCUSSION

Our empirical observations propose that we should explore 2D annotation-based pre-training instead of SSL for 3DHPSE. However, SSL may still have an advantage over 2D annotation-based pre-

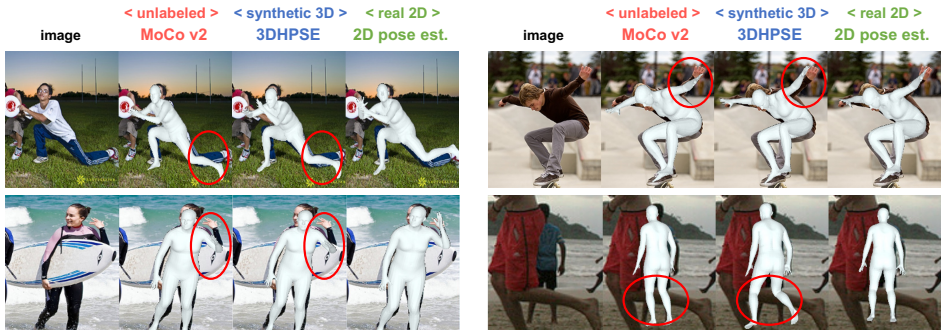


Figure 5: Qualitative comparison among different pre-training schemes. We highlighted their representative failure cases with red circles.



Figure 6: Feature attention visualization of PARE (Kocabas et al., 2021) for different human parts.

training in the aspect of labeling costs. In this regard, we answer two questions that could help future 3DHPSE researchers to choose their pre-training strategies.

(i) *Does SSL entail a zero cost?* No. It is not true in the aspect of data collection. Collecting, cleaning, and curating data for SSL demand resources (Russakovsky et al., 2015; He et al., 2019; Kotar et al., 2021). More importantly, the current SSL methods for 3DHPSE (Spurr et al., 2021; Zimmermann et al., 2021) assume a human to be centered in an input image, which is an unrealistic setting for in-the-wild images without bounding box labels. Thus, we should consider the labeling cost of bounding boxes when using SSL (Purushwalkam & Gupta, 2020; Goyal et al., 2021; El-Nouby et al., 2021). Further discussion is provided in Section B of Appendix.

(ii) *Is SSL efficient than 2D annotation-based pre-training?* No. SSL pre-trains on massive unlabeled data, which involves high computational costs. It often results in order of magnitude more computation than the supervised counterparts (Hénaff et al., 2021). In addition, due to double feature encoders and complex feature contrasting mechanism, SSL takes more time than 2D annotation-based pre-training to pre-train on the same amount of pre-training data. Pre-training ResNet-50 (He et al., 2016) with PeCLR (Spurr et al., 2021), MoCo v2 (Chen et al., 2020c), and the 2D pose estimator on MSCOCO took 110, 226, and 14 hours respectively, with the four RTX 2080Ti GPUs.

6 CONCLUSION

We have investigated different approaches for pre-training a 3DHPSE backbone. SSL, which has recently become the major trend in the community, has been thoroughly inspected. 2D annotation-based pre-training and synthetic data pre-training have also been experimented, since they share the similar motivation of reducing labeling costs and transferring useful representations to 3DHPSE. We experimented with multiple methods of each approach on multiple benchmarks to not draw a conclusion valid in a limited setting. Please also refer to Section D to confirm that our observations on the three pre-training approaches are preserved regardless of a 3DHPSE mesh regressor. Our empirical results show that 1) SSL is yet to replace the de facto paradigm of the ImageNet classification pre-training, and 2) 2D annotation-based pre-training can effectively transfer the knowledge to 3DHPSE, despite the least amount of pre-training data. We believe our findings, analysis, and discussion will significantly influence future research on pre-training for 3DHPSE.

Acknowledgements. This work was supported in part by the IITP grants [No.2021-0-01343, Artificial Intelligence Graduate School Program (Seoul National University), No.2022-0-00156, No. 2021-0-02068, and No.2022-0-00156], and the NRF grant [No. 2021M3A9E4080782] funded by the Korea government (MSIT), and AIRS Company in Hyundai Motor Company & Kia Corporation through HMC/KIA-SNU AI Consortium Fund.

REFERENCES

- Mykhaylo Andriluka, Leonid Pishchulin, Peter Gehler, and Bernt Schiele. 2d human pose estimation: New benchmark and state of the art analysis. In *CVPR*, 2014.
- Fabien Baradel, Thibault Groueix, Philippe Weinzaepfel, Romain Brégier, Yannis Kalantidis, and Grégory Rogez. Leveraging mocap data for human mesh recovery. In *3DV*, 2021.
- Federica Bogo, Angjoo Kanazawa, Christoph Lassner, Peter Gehler, Javier Romero, and Michael J Black. Keep it SMPL: Automatic estimation of 3D human pose and shape from a single image. In *ECCV*, 2016.
- Zhongang Cai, Mingyuan Zhang, Jiawei Ren, Chen Wei, Daxuan Ren, Jiatong Li, Zhengyu Lin, Haiyu Zhao, Shuai Yi, Lei Yang, et al. Playing for 3d human recovery. *arXiv*, 2021.
- Zhe Cao, Tomas Simon, Shih-En Wei, and Yaser Sheikh. Realtime multi-person 2d pose estimation using part affinity fields. In *CVPR*, 2017.
- Mathilde Caron, Ishan Misra, Julien Mairal, Priya Goyal, Piotr Bojanowski, and Armand Joulin. Unsupervised learning of visual features by contrasting cluster assignments. In *NeurIPS*, 2020.
- Joao Carreira and Andrew Zisserman. Quo vadis, action recognition? a new model and the kinetics dataset. In *CVPR*, 2017.
- Ting Chen, Simon Kornblith, Mohammad Norouzi, and Geoffrey Hinton. A simple framework for contrastive learning of visual representations. In *ICML*, 2020a.
- Ting Chen, Simon Kornblith, Kevin Swersky, Mohammad Norouzi, and Geoffrey E Hinton. Big self-supervised models are strong semi-supervised learners. In *NeurIPS*, 2020b.
- Xinlei Chen and Kaiming He. Exploring simple siamese representation learning. *arXiv preprint arXiv:2011.10566*, 2020.
- Xinlei Chen, Haoqi Fan, Ross Girshick, and Kaiming He. Improved baselines with momentum contrastive learning. *arXiv preprint arXiv:2003.04297*, 2020c.
- Hongsuk Choi, Gyeongsik Moon, and Kyoung Mu Lee. Pose2Mesh: Graph convolutional network for 3D human pose and mesh recovery from a 2D human pose. In *ECCV*, 2020.
- Hongsuk Choi, Gyeongsik Moon, Ju Yong Chang, and Kyoung Mu Lee. Beyond static features for temporally consistent 3d human pose and shape from a video. In *CVPR*, 2021.
- Hongsuk Choi, Gyeongsik Moon, JoonKyu Park, and Kyoung Mu Lee. Learning to estimate robust 3d human mesh from in-the-wild crowded scenes. In *CVPR*, 2022.
- Mickael Cormier, Fabian Röpke, Thomas Golda, and Jürgen Beyerer. Interactive labeling for human pose estimation in surveillance videos. In *ICCV workshop*, 2021.
- Alaaeldin El-Nouby, Gautier Izacard, Hugo Touvron, Ivan Laptev, Hervé Jegou, and Edouard Grave. Are large-scale datasets necessary for self-supervised pre-training? *arXiv preprint arXiv:2112.10740*, 2021.
- Ross Girshick, Jeff Donahue, Trevor Darrell, and Jitendra Malik. Rich feature hierarchies for accurate object detection and semantic segmentation. In *CVPR*, 2014.
- Priya Goyal, Mathilde Caron, Benjamin Lefaudeaux, Min Xu, Pengchao Wang, Vivek Pai, Mannat Singh, Vitaliy Liptchinsky, Ishan Misra, Armand Joulin, et al. Self-supervised pretraining of visual features in the wild. *arXiv preprint arXiv:2103.01988*, 2021.

- Jean-Bastien Grill, Florian Strub, Florent Alché, Corentin Tallec, Pierre Richemond, Elena Buchatskaya, Carl Doersch, Bernardo Avila Pires, Zhaohan Guo, Mohammad Gheshlaghi Azar, et al. Bootstrap your own latent-a new approach to self-supervised learning. In *NeurIPS*, 2020.
- Rıza Alp Güler, Natalia Neverova, and Iasonas Kokkinos. Densepose: Dense human pose estimation in the wild. In *CVPR*, 2018.
- Kaiming He, Xiangyu Zhang, Shaoqing Ren, and Jian Sun. Deep residual learning for image recognition. In *CVPR*, 2016.
- Kaiming He, Georgia Gkioxari, Piotr Dollár, and Ross Girshick. Mask r-cnn. In *ICCV*, 2017.
- Kaiming He, Ross Girshick, and Piotr Dollár. Rethinking imagenet pre-training. In *ICCV*, 2019.
- Kaiming He, Haoqi Fan, Yuxin Wu, Saining Xie, and Ross Girshick. Momentum contrast for unsupervised visual representation learning. In *CVPR*, 2020.
- Olivier J Hénaff, Skanda Koppula, Jean-Baptiste Alayrac, Aaron van den Oord, Oriol Vinyals, and João Carreira. Efficient visual pretraining with contrastive detection. In *ICCV*, 2021.
- Catalin Ionescu, Dragos Papava, Vlad Olaru, and Cristian Sminchisescu. Human3.6m: Large scale datasets and predictive methods for 3d human sensing in natural environments. *TPAMI*, 2014.
- Sam Johnson and Mark Everingham. Clustered pose and nonlinear appearance models for human pose estimation. In *BMVC*, 2010.
- Hanbyul Joo, Natalia Neverova, and Andrea Vedaldi. Exemplar fine-tuning for 3d human model fitting towards in-the-wild 3d human pose estimation. In *3DV*, 2021.
- Angjoo Kanazawa, Michael J Black, David W Jacobs, and Jitendra Malik. End-to-end recovery of human shape and pose. In *CVPR*, 2018.
- Angjoo Kanazawa, Jason Y Zhang, Panna Felsen, and Jitendra Malik. Learning 3d human dynamics from video. In *CVPR*, 2019.
- Prannay Khosla, Piotr Teterwak, Chen Wang, Aaron Sarna, Yonglong Tian, Phillip Isola, Aaron Maschinot, Ce Liu, and Dilip Krishnan. Supervised contrastive learning. In *NeurIPS*, 2020.
- Muhammed Kocabas, Nikos Athanasiou, and Michael J Black. VIBE: Video inference for human body pose and shape estimation. In *CVPR*, 2020.
- Muhammed Kocabas, Chun-Hao P Huang, Otmar Hilliges, and Michael J Black. Pare: Part attention regressor for 3d human body estimation. In *ICCV*, 2021.
- Nikos Kolotouros, Georgios Pavlakos, Michael J Black, and Kostas Daniilidis. Learning to reconstruct 3D human pose and shape via model-fitting in the loop. In *ICCV*, 2019a.
- Nikos Kolotouros, Georgios Pavlakos, and Kostas Daniilidis. Convolutional mesh regression for single-image human shape reconstruction. In *CVPR*, 2019b.
- Klemen Kotar, Gabriel Ilharco, Ludwig Schmidt, Kiana Ehsani, and Roozbeh Mottaghi. Contrasting contrastive self-supervised representation learning pipelines. In *ICCV*, 2021.
- Alex Krizhevsky, Ilya Sutskever, and Geoffrey E Hinton. Imagenet classification with deep convolutional neural networks. *CACM*, 2017.
- Kevin Lin, Lijuan Wang, and Zicheng Liu. End-to-end human pose and mesh reconstruction with transformers. In *CVPR*, 2021.
- Tsung-Yi Lin, Michael Maire, Serge Belongie, James Hays, Pietro Perona, Deva Ramanan, Piotr Dollár, and C Lawrence Zitnick. Microsoft coco: Common objects in context. In *ECCV*, 2014.
- Buyu Liu and Vittorio Ferrari. Active learning for human pose estimation. In *ICCV*, 2017.
- Matthew Loper, Naureen Mahmood, Javier Romero, Gerard Pons-Moll, and Michael J. Black. SMPL: A skinned multi-person linear model. *ACM TOG*, 2015.

- Dhruv Mahajan, Ross Girshick, Vignesh Ramanathan, Kaiming He, Manohar Paluri, Yixuan Li, Ashwin Bharambe, and Laurens Van Der Maaten. Exploring the limits of weakly supervised pretraining. In *ECCV*, 2018.
- Dushyant Mehta, Helge Rhodin, Dan Casas, Pascal Fua, Oleksandr Sotnychenko, Weipeng Xu, and Christian Theobalt. Monocular 3d human pose estimation in the wild using improved cnn supervision. In *3DV*, 2017.
- Dushyant Mehta, Oleksandr Sotnychenko, Franziska Mueller, Weipeng Xu, Srinath Sridhar, Gerard Pons-Moll, and Christian Theobalt. Single-shot multi-person 3d pose estimation from monocular rgb. In *3DV*, 2018.
- Gyeongsik Moon and Kyoung Mu Lee. I2L-MeshNet: Image-to-Lixel prediction network for accurate 3D human pose and mesh estimation from a single RGB image. In *ECCV*, 2020.
- Gyeongsik Moon, Hongsuk Choi, and Kyoung Mu Lee. Accurate 3d hand pose estimation for whole-body 3d human mesh estimation. In *CVPR workshop*, 2022a.
- Gyeongsik Moon, Hongsuk Choi, and Kyoung Mu Lee. Neuralannot: Neural annotator for 3d human mesh training sets. In *CVPR workshop*, 2022b.
- Hui En Pang, Zhongang Cai, Lei Yang, Tianwei Zhang, and Ziwei Liu. Benchmarking and analyzing 3d human pose and shape estimation beyond algorithms. In *NeurIPS*, 2022.
- Dim P Papadopoulos, Jasper RR Uijlings, Frank Keller, and Vittorio Ferrari. Extreme clicking for efficient object annotation. In *ICCV*, 2017.
- Adam Paszke, Sam Gross, Soumith Chintala, Gregory Chanan, Edward Yang, Zachary DeVito, Zeming Lin, Alban Desmaison, Luca Antiga, and Adam Lerer. Automatic differentiation in pytorch. In *NeurIPS*, 2017.
- Priyanka Patel, Chun-Hao P Huang, Joachim Tesch, David T Hoffmann, Shashank Tripathi, and Michael J Black. Agora: Avatars in geography optimized for regression analysis. In *CVPR*, 2021.
- Georgios Pavlakos, Vasileios Choutas, Nima Ghorbani, Timo Bolkart, Ahmed AA Osman, Dimitrios Tzionas, and Michael J Black. Expressive body capture: 3d hands, face, and body from a single image. In *CVPR*, 2019.
- Senthil Purushwalkam and Abhinav Gupta. Demystifying contrastive self-supervised learning: Invariances, augmentations and dataset biases. In *NeurIPS*, 2020.
- Helge Rhodin, Mathieu Salzmann, and Pascal Fua. Unsupervised geometry-aware representation for 3d human pose estimation. In *ECCV*, 2018.
- Helge Rhodin, Victor Constantin, Isinsu Katircioglu, Mathieu Salzmann, and Pascal Fua. Neural scene decomposition for multi-person motion capture. In *CVPR*, 2019.
- Yu Rong, Ziwei Liu, Cheng Li, Kaidi Cao, and Chen Change Loy. Delving deep into hybrid annotations for 3d human recovery in the wild. In *ICCV*, 2019.
- Olga Russakovsky, Jia Deng, Hao Su, Jonathan Krause, Sanjeev Satheesh, Sean Ma, Zhiheng Huang, Andrej Karpathy, Aditya Khosla, Michael Bernstein, et al. Imagenet large scale visual recognition challenge. *IJCV*, 2015.
- Adrian Spurr, Aneesh Dahiya, Xi Wang, Xucong Zhang, and Otmar Hilliges. Self-supervised 3d hand pose estimation from monocular rgb via contrastive learning. In *ICCV*, 2021.
- Ke Sun, Bin Xiao, Dong Liu, and Jingdong Wang. Deep high-resolution representation learning for human pose estimation. In *CVPR*, 2019.
- Atharva Tendle and Mohammad Rashedul Hasan. A study of the generalizability of self-supervised representations. *MLA*, 2021.
- Gül Varol, Javier Romero, Xavier Martin, Naureen Mahmood, Michael J. Black, Ivan Laptev, and Cordelia Schmid. Learning from synthetic humans. In *CVPR*, 2017.

- Timo von Marcard, Roberto Henschel, Michael Black, Bodo Rosenhahn, and Gerard Pons-Moll. Recovering accurate 3d human pose in the wild using imus and a moving camera. In *ECCV*, 2018.
- Bin Xiao, Haiping Wu, and Yichen Wei. Simple baselines for human pose estimation and tracking. In *ECCV*, 2018.
- Jason Yosinski, Jeff Clune, Anh Nguyen, Thomas Fuchs, and Hod Lipson. Understanding neural networks through deep visualization. In *ICML workshop*, 2015.
- Hongwen Zhang, Yating Tian, Xinchu Zhou, Wanli Ouyang, Yebin Liu, Limin Wang, and Zhenan Sun. Pymaf: 3d human pose and shape regression with pyramidal mesh alignment feedback loop. In *ICCV*, 2021a.
- Hongwen Zhang, Yating Tian, Xinchu Zhou, Wanli Ouyang, Yebin Liu, Limin Wang, and Zhenan Sun. PyMAF: 3D human pose and shape regression with pyramidal mesh alignment feedback loop. In *ICCV*, 2021b.
- Christian Zimmermann, Duygu Ceylan, Jimei Yang, Bryan Russell, Max Argus, and Thomas Brox. Freihand: A dataset for markerless capture of hand pose and shape from single rgb images. In *ICCV*, 2019.
- Christian Zimmermann, Max Argus, and Thomas Brox. Contrastive representation learning for hand shape estimation. In *GCPR*, 2021.

APPENDIX

In this supplementary material, we provide more experiments and discussions that could not be included in the main text due to the lack of pages. The contents are summarized below:

A - Effects of SSL and 2D annotation-based pre-training on different amounts of data; InstaVariety(246K) (Kanazawa et al., 2019) and MPII(25K) (Andriluka et al., 2014) are experimented in addition to MSCOCO(150K) (Lin et al., 2014).

B - Discussion about labeling costs of SSL and 2D annotation-based pre-training

C - Effects of different pre-training approaches, when fine-tuned on different sizes of human data (30% and 60% of (Human3.6M (Ionescu et al., 2014) + MSCOCO (Lin et al., 2014)))

D - Effects of different human mesh regressors.

A EFFECTS OF PRE-TRAINING ON DIFFERENT AMOUNTS OF DATA

SSL is known to require large-scale pre-training data to be effective (He et al., 2020). In this regard, we apply PeCLR (Spurr et al., 2021) and MoCo v2 (Chen et al., 2020c) on InstaVariety(246K) (Kanazawa et al., 2019), which is $1.64\times$ bigger than MSCOCO(150K) (Lin et al., 2014). Interestingly, pre-training on InstaVariety consistently shows worse accuracy in all benchmarks as shown in Table 4. If we use less fine-tuning data, the accuracy gap is increased, except PeCLR on Human3.6M. We think the seemingly contradictory results come from the noisy bounding box used to crop a human from an image. The bounding box of a human in InstaVariety is calculated by measuring minimum and maximum x, y locations of OpenPose (Cao et al., 2017)’s 2D pose estimation. Since the estimated values inevitably have errors, the bounding box obtained from them may not produce a human-centered image. Thus, the input distribution could be severely different during pre-training and fine-tuning, which could lead to counter-intuitive results.

We also provide the results of 2D pose estimation pre-training on MPII(25K) (Andriluka et al., 2014). Despite much less pre-training data, 2D pose estimation pre-training achieves comparable accuracy to that of pre-training MSCOCO. This shows the cost-effectiveness of 2D pose estimation pre-training, which is further discussed in the next section.

Table 4: Effects of pre-training on different amounts of data. InstaVariety(246K) (Kanazawa et al., 2019), MSCOCO(150K) (Lin et al., 2014), and MPII(25K) (Andriluka et al., 2014) are used for pre-training. The red and blue colors indicate the first and second best scores, respectively.

fine-tuning data	pre-training data	pre-training method	3DPW PA-MPJPE↓	H36M PA-MPJPE↓	MuPoTS 3DPCK↑
H36M+ MSCOCO (100%)	InstaVariety (unlabeled)	PeCLR (Spurr et al., 2021)	57.45	51.17	66.77
		MoCo v2 (Chen et al., 2020c)	57.28	51.14	67.53
	MSCOCO (unlabeled)	PeCLR (Spurr et al., 2021)	57.27	49.84	66.88
		MoCo v2 (Chen et al., 2020c)	56.35	50.06	66.95
	MSCOCO	2D pose est.	53.34	44.89	69.04
	MPII	2D pose est.	54.71	46.12	67.61
H36M+ MSCOCO (10%)	InstaVariety (unlabeled)	PeCLR (Spurr et al., 2021)	74.65	64.77	56.51
		MoCo v2 (Chen et al., 2020c)	76.49	70.42	58.72
	MSCOCO (unlabeled)	PeCLR (Spurr et al., 2021)	71.24	66.58	60.16
		MoCo v2 (Chen et al., 2020c)	66.93	62.06	61.36
	MSCOCO	2D pose est.	56.92	55.31	67.12
	MPII	2D pose est.	62.71	58.39	62.57

B DISCUSSION ABOUT LABELING COSTS OF SSL AND 2D ANNOTATION-BASED PRE-TRAINING

Some could value SSL on bounding box-labeled human data more than 2D annotation-based pre-training, despite the experimental results of the main text. For example, assuming less fine-tuning data like the main text’s Table 6, MoCo v2 (Chen et al., 2020c) may be a more attractive option than the 2D pose estimation pre-training, considering that bounding box annotations take less cost than 2D pose annotations. In this context, we analyze the cost-effectiveness of different pre-training approaches by comparing the annotation cost in terms of annotation time.

Table 5 supports that the 2D pose estimation pre-training is much more cost-effective, given the similar annotation time. The state-of-the-art object annotation paper (Papadopoulos et al., 2017) reported 7 seconds per one bounding box annotation. We assume that the same time would take for a human bounding box. Liu et al. (Liu & Ferrari, 2017) reported 1.5 seconds per one human key point. Since a person in MPII (Andriluka et al., 2014) images have 14 key points, we can assume that the annotation time is 21 seconds per person. Cormier et al. (Cormier et al., 2021) reported 42.8 seconds per bounding box and pose of one person. We take the number of Cormier et al. (Cormier et al., 2021) in Table 5.

Table 5: Comparison between cost-effectiveness of SSL on bounding box-labeled data and 2D pose estimation pre-training.

pre-training method	pre-training data	annotation time	3DPW PA-MPJPE↓	H36M PA-MPJPE↓	MuPoTS 3DPCK↑
MoCo v2 (Chen et al., 2020c)	MSCOCO (150K) (unlabeled)	150K×7s=1050Ks	56.35	50.06	66.95
2D pose est.	MPII (25K)	25K×42.8s=1070Ks	53.34	44.89	69.04

C FINE-TUNING ON DIFFERENT SIZES OF HUMAN DATA

We explore the effects of different pre-training approaches in different semi-supervised settings by varying sizes of fine-tuning data. Experimental results of using 10%, 30%, 60%, and 100% fine-tuning data of (Human3.6M (Ionescu et al., 2014) + MSCOCO (Lin et al., 2014)) are shown in Table 6 and Figure 7. SSL starts to surpass the random initialization baseline when fine-tuning data is reduced to 30%. Synthetic data pre-training also shows a similar tendency. Only 2D annotation-based pre-training consistently outperforms the random initialization baseline, and the accuracy margin is enlarged as the fine-tuning data reduces.

Table 6: 3DHPSE evaluation results on pre-training schemes with **different sizes of human data**. We report the best accuracy of each scheme on 3DPW, Human3.6M, and MuPoTS-3D dataset. The **red** and **blue** colors indicate the first and second best scores, respectively.

fine-tuning data	pre-training data	pre-training method	3DPW PA-MPJPE↓	H36M PA-MPJPE↓	MuPoTS 3DPCK↑
H36M+ MSCOCO (100%)	-	random init.	56.37	52.72	67.12
	ImageNet (labeled)	classification	55.65	48.36	67.76
	MSCOCO (unlabeled)	PeCLR (Spurr et al., 2021)	57.27	49.84	66.88
		MoCo v2 (Chen et al., 2020c)	56.35	50.06	66.95
	AGORA SURREAL	3DHPSE	56.77	51.96	67.80
			56.45	52.51	67.65
	MSCOCO	DensePose est. 2D pose est.	54.16 53.34	49.18 44.89	68.43 69.04
H36M+ MSCOCO (60%)	-	random init.	57.31	50.61	67.30
	ImageNet (labeled)	classification	55.63	51.87	67.34
	MSCOCO (unlabeled)	PeCLR (Spurr et al., 2021)	59.17	52.14	65.80
		MoCo v2 (Chen et al., 2020c)	58.57	52.34	66.63
	AGORA SURREAL	3DHPSE	57.23	53.99	68.87
			57.69	53.10	66.47
	MSCOCO	DensePose est. 2D pose est.	54.80 54.41	49.38 52.03	68.44 67.91
H36M+ MSCOCO (30%)	-	random init.	62.40	56.49	63.20
	ImageNet (labeled)	classification	57.85	53.02	65.74
	MSCOCO (unlabeled)	PeCLR (Spurr et al., 2021)	63.43	55.90	63.66
		MoCo v2 (Chen et al., 2020c)	60.95	55.09	64.96
	AGORA SURREAL	3DHPSE	60.50	56.05	67.43
			57.92	53.93	68.74
	MSCOCO	DensePose est. 2D pose est.	55.44 53.94	52.37 47.39	68.40 68.56
H36M+ MSCOCO (10%)	-	random init.	73.37	67.59	57.32
	ImageNet (labeled)	classification	63.29	58.79	62.75
	MSCOCO (unlabeled)	PeCLR (Spurr et al., 2021)	71.24	66.58	60.16
		MoCo v2 (Chen et al., 2020c)	66.93	62.06	61.36
	AGORA SURREAL	3DHPSE	64.71	63.17	65.73
			62.51	59.10	64.50
	MSCOCO	DensePose est. 2D pose est.	57.33 56.92	54.46 55.31	68.02 67.12

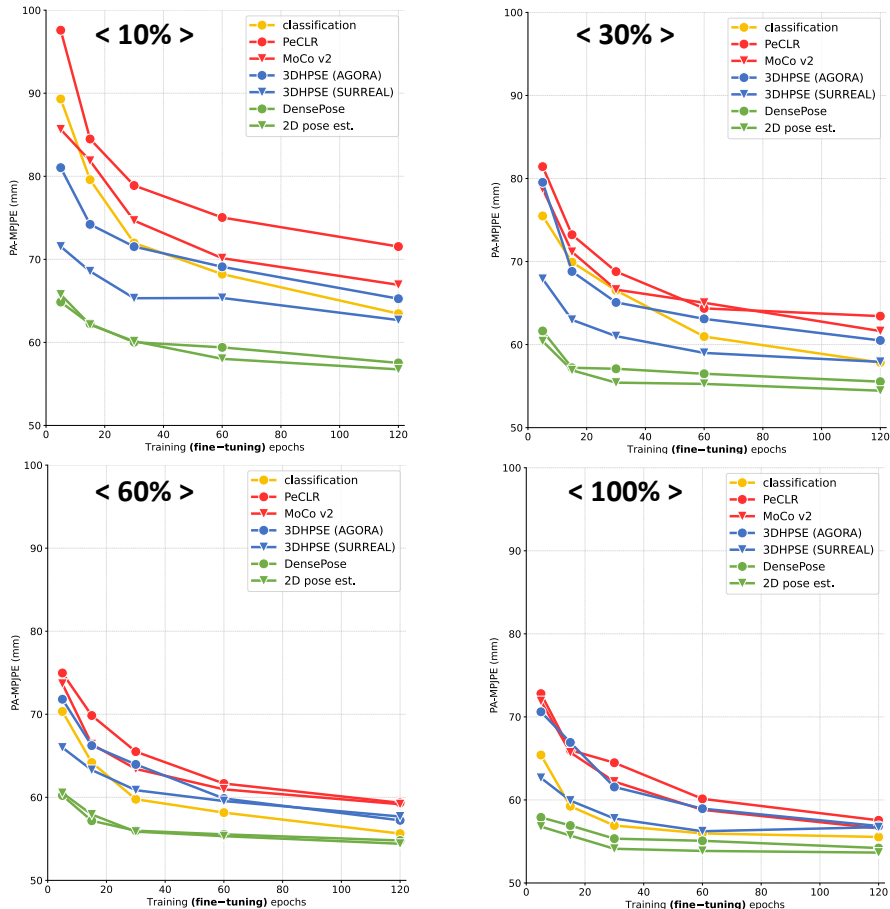


Figure 7: Learning curves of PA-MPJPE on 3DPW in the fine-tuning stage with different weights pre-trained on **different sizes of human data** by different pre-training methods.

D EFFECTS OF DIFFERENT HUMAN MESH REGRESSORS

In Table 7 and Table 8, we experiment with different human mesh regressors (Kolotouros et al., 2019a; Zhang et al., 2021a; Moon et al., 2022a; Moon & Lee, 2020) that have distinct architectures and achieved state-of-the-art accuracy recently. The best-performing methods of SSL, synthetic data pre-training, and 2D annotation-based pre-training are used to compare. Overall, the same tendency is observed. SSL and synthetic data pre-training underperform the classification baseline, while 2D annotation-based pre-training outperforms it in multiple 3DHPSE benchmarks. This shows that our observations are not limited to a single 3DHPSE method but can generalize to different methods. The notable result is that I2L-MeshNet (Moon & Lee, 2020) produces overall the same accuracy regardless of the pre-training approaches. We conjecture that the different tendency of I2L-MeshNet comes from its architecture and target representation. While other human mesh regressors estimate the SMPL (Loper et al., 2015) parameters with MLP layers at the end of their networks, I2L-MeshNet directly regresses 2.5D locations of mesh vertices in a fully convolutional manner. The 2.5D representation expresses the xy locations of mesh vertices in the image pixel space and the z location as root joint-relative depth. As a result, the accuracy of I2L-MeshNet depends on the segmentation of a human from a cropped human-centric image. This partially posits the problem of 3DHPSE to the foreground estimation, which may less demand on learning complex priors about humans, such as 3D human body articulation.

Table 7: Effects of different human mesh regressors. We utilize SPIN (Kolotouros et al., 2019a), PyMAF (Zhang et al., 2021b), Pose2Pose (Moon et al., 2022a), and I2L-MeshNet (Moon & Lee, 2020) as regressors. We use full data (Human3.6M and MSCOCO) data for fine-tuning. The red and blue colors indicate the first and second best scores, respectively.

regressor	pre-training data	pre-training method	3DPW PA-MPJPE↓	H36M PA-MPJPE↓	MuPoTS 3DPCK↑
SPIN	ImageNet	classification	64.73	51.21	66.32
	MSCOCO	MoCo v2 (Chen et al., 2020c)	64.98	57.04	63.98
	AGORA	3DHPSE	66.00	55.51	64.99
	MSCOCO	2D pose est.	59.78	51.29	66.75
PyMAF	ImageNet	classification	60.37	67.23	68.19
	MSCOCO	MoCo v2 (Chen et al., 2020c)	64.09	69.49	65.49
	AGORA	3DHPSE	65.60	71.63	66.72
	MSCOCO	2D pose est.	59.04	69.53	70.46
Pose2Pose	ImageNet	classification	57.07	44.32	67.80
	MSCOCO	MoCo v2 (Chen et al., 2020c)	62.11	53.91	65.33
	AGORA	3DHPSE	61.00	51.28	66.51
	MSCOCO	2D pose est.	56.78	41.79	68.54
I2L-MeshNet (lixel stage)	ImageNet	classification	60.74	39.42	70.76
	MSCOCO	MoCo v2 (Chen et al., 2020c)	61.11	38.34	71.50
	AGORA	3DHPSE	60.48	39.62	71.73
	MSCOCO	2D pose est.	60.49	38.99	71.88

Table 8: Effects of different human mesh regressors in **semi-supervised setting**. We utilize SPIN (Kolotouros et al., 2019a), PyMAF (Zhang et al., 2021b), Pose2Pose (Moon et al., 2022a), and I2L-MeshNet (Moon & Lee, 2020) as regressors. We use 10% of (Human3.6M and MSCOCO) data for fine-tuning. The red and blue colors indicate the first and second best scores, respectively.

regressor	pre-training data	pre-training method	3DPW PA-MPJPE↓	H36M PA-MPJPE↓	MuPoTS 3DPCK↑
SPIN	ImageNet	classification	78.99	75.97	55.00
	MSCOCO	MoCo v2 (Chen et al., 2020c)	86.85	81.63	48.47
	AGORA	3DHPSE	83.73	82.76	54.04
	MSCOCO	2D pose est.	64.57	64.96	65.51
PyMAF	ImageNet	classification	67.64	73.62	63.76
	MSCOCO	MoCo v2 (Chen et al., 2020c)	71.90	80.43	58.69
	AGORA	3DHPSE	69.65	81.71	62.04
	MSCOCO	2D pose est.	59.41	73.84	68.91
Pose2Pose	ImageNet	classification	66.85	61.06	64.79
	MSCOCO	MoCo v2 (Chen et al., 2020c)	74.25	73.33	59.61
	AGORA	3DHPSE	69.66	67.04	63.02
	MSCOCO	2D pose est.	57.97	54.91	68.45
I2L-MeshNet (lixel stage)	ImageNet	classification	61.47	50.74	71.97
	MSCOCO	MoCo v2 (Chen et al., 2020c)	62.38	51.88	72.28
	AGORA	3DHPSE	61.43	51.72	72.15
	MSCOCO	2D pose est.	62.05	51.21	71.50